Copy No. 3

RM No. L8H12

RESTRICTED

NACA RM No. L8H12

UNCLASSIFIED

NACA

RESEARCH MEMORANDUM

YAW CHARACTERISTICS OF A 52° SWEPTBACK WING OF NACA 64_1-112 SECTION WITH A FUSELAGE AND WITH LEADING-EDGE AND SPLIT FLAPS AT REYNOLDS NUMBERS FROM 1.93×10^6 to 6.00×10^6

By

Reino J. Salmi

Langley Aeronautical Laboratory
Langley Field, Va.

NATIONAL ADVISORY COMMITTEE FOR AERONAUTICS

WASHINGTON

November 8, 1948

RESTRICTED

NACA RM No. L8H12

NATIONAL ADVISORY COMMITTEE FOR AERONAUTICS

RESEARCH MEMORANDUM

YAW CHARACTERISTICS OF A 52° SWEPTBACK WING OF NACA 64_1-112 SECTION WITH A FUSELAGE AND WITH LEADING-EDGE AND SPLIT FLAPS AT REYNOLDS NUMBERS FROM 1.93×10^6 to 6.00×10^6

By Reino J. Salmi

SUMMARY

Low-speed tests were made in the Langley 19-foot pressure tunnel to determine the aerodynamic characteristics in yaw of a 52° sweptback wing of aspect ratio 2.88 and taper ratio 0.625 with NACA 64_1-112 airfoil sections. The tests included an investigation of the effects on the lateral stability of a fuselage and leading-edge and split flaps. Air-stream surveys were conducted to determine the sidewash characteristics in the region of a vertical tail. The data were obtained at Reynolds numbers of 1.93×10^6, 4.35×10^6, and 6.00×10^6.

The maximum value of the effective-dihedral parameter obtained for the plain wing was about 0.0043 at a lift coefficient of 0.95. At higher lift coefficients the dihedral effect decreased rapidly and became negative. The combination of leading-edge flaps, split flaps and fences, extended the range of increase of the effective-dihedral parameter with lift coefficient up to the maximum lift coefficient. The plain wing was directionally stable up to a lift coefficient of 0.76 and this was increased to higher lift coefficients when the leading-edge flaps and split flaps were deflected, but in all cases the wing was directionally unstable near the maximum lift. The low-wing combination and the high-wing combination had lower and higher values of effective dihedral, respectively, than the plain wing. The magnitudes of the differences were of the same order as had been experienced on other swept and unswept wings. The scale effect was appreciable in the Reynolds number range from 1.93×10^6 to 4.35×10^6 but was moderate in the range from 4.35×10^6 to 6.00×10^6.

INTRODUCTION

Investigations of the lateral stability of sweptback wings have shown that except at low angles of attack, the lateral-stability parameters are primarily dependent on the stalling characteristics of the wing. The stalling characteristics, in turn, are determined by such factors as the airfoil section employed, the angle of wing sweep, the aspect ratio, the Reynolds number, the high-lift devices used, and the interference effect of other airplane components such as a fuselage. A general investigation is being conducted in the Langley 19-foot pressure tunnel to separate the interrelated actions of these various factors and to study their effects on the static lateral stability of swept wings. Previous investigations have been conducted on wings of 42° sweepback and are summarized in references 1 and 2.

The present investigation has been conducted to determine the effects of Reynolds number, leading-edge and split flaps, and a fuselage on the lateral-stability characteristics of a 52° sweptback wing. Airstream surveys in the region of a vertical tail were also made to ascertain the effects of low aspect ratio and large sweepback angle on the sidewash characteristics. The longitudinal characteristics of the basic wing and the wing with split flaps have been presented in reference 3.

COEFFICIENTS AND SYMBOLS

The data are referred to a system of axes shown in figure 1. All moments for the wing-fuselage combinations are referred to the assumed center of gravity, which is located on the fuselage center line and in a plane normal to the fuselage center line that passes through the quarter-chord point of the mean aerodynamic chord. The moment data for the wing alone are referred to the quarter-chord point of the mean aerodynamic chord projected to the plane of symmetry. Standard NACA symbols are used, which are defined as follows:

C_L	lift coefficient $\left(\frac{\text{Lift}}{qS}\right)$
$C_{L_{max}}$	maximum lift coefficient
C_D	drag coefficient (D/qS)
C_X	longitudinal-force coefficient (X/qS)
C_Y	lateral-force coefficient (Y/qS)
C_m	pitching-moment coefficient $(M/qS\bar{c})$
C_l	rolling-moment coefficient (L/qSb)

C_n yawing-moment coefficient (N/qSb)

C_{l_ψ} effective-dihedral parameter $(\partial C_l/\partial\psi)$

C_{n_ψ} directional-stability parameter $(\partial C_n/\partial\psi)$

C_{Y_ψ} lateral-force parameter $(\partial C_Y/\partial\psi)$

Lift = -Z

D drag, -X at zero yaw

X longitudinal force

Y lateral force

Z vertical force

L rolling moment

M pitching moment

N yawing moment

α angle of attack of wing chord line, degrees

ψ angle of yaw, positive when right wing is back, degrees

S wing area

c local chord parallel to plane of symmetry

$\bar{c}$ mean aerodynamic chord measured parallel to plane of symmetry $\left(\frac{2}{S}\int_0^{b/2} c^2\,dy\right)$

b wing span

y spanwise coordinate

q free-stream dynamic pressure $\left(\frac{1}{2}\rho V^2\right)$

q_t dynamic pressure at region of tail

V	free-stream velocity
ρ	mass density of air
R	Reynolds number $(\rho V\bar{c}/\mu)$
μ	coefficient of viscosity of air
M	Mach number (V/a)
a	velocity of sound
h	height above fuselage center line, percent $\bar{c}$
h'	height above wing chord plane, percent $\bar{c}$
σ	sidewash angle (angle between direction of air flow and tunnel center line measured in the XY-plane, positive when the angle of attack at the vertical tail is decreased, when the model is at a positive angle of yaw), degrees

APPARATUS AND TESTS

Apparatus

The dimensions and details of the model are shown in figure 2. The wing had a sweepback angle of 52.05° along the leading edge and had NACA 64_1-112 airfoil sections normal to the 0.282 chord line. The aspect ratio and taper ratio were 2.88 and 0.625, respectively. No dihedral or twist were incorporated in the wing. The construction was of laminated mahogany reinforced by steel plates, and the wing surfaces were lacquered and sanded to an aerodynamically smooth finish.

The fuselage was circular in cross section with a fineness ratio of 10.2. The diameter was constant along a section which extended from about 28.1 percent to 65.5 percent of its length. The wing was mounted on the fuselage to form high-wing, low-wing, and midwing combinations. An incidence of 2° was maintained for all combinations.

The leading-edge flaps were made of curved sheet steel welded to a $\frac{1}{2}$-inch-diameter steel tube (fig. 3). They extended from 40 percent to 97.5 percent of the semispan and were deflected 50° from the chord plane extended, when measured in a plane normal to 0.282-chord-line

edge. The flap chord was constant at 3.19 inches, measured normal to the 0.282 chord line. The split flaps were made of sheet steel and extended over the inboard 50 percent of the span. The chord was 20 percent of the wing chord normal to the 0.282 chord line, and the flaps were deflected 60° from the wing lower surface measured normal to the 0.282 chord line.

Upper-surface fences were used on the model whenever the leading-edge flaps were deflected (fig. 3). The fences were made from sheet steel and were mounted parallel with the model center line at a wing station 45 percent of the semispan, measured from the plane of symmetry. The fences were of constant height, being 60 percent of the maximum thickness of the local airfoil section, and extended over the rear 95 percent of the airfoil chord.

Figure 4 shows the model mounted on the single-support system in the Langley 19-foot pressure tunnel. This installation allows both the angle of attack and angle of yaw to be varied while the tunnel is in operation.

Tests

The data were obtained at Reynolds numbers of 1.93×10^6, 4.35×10^6, and 6.00×10^6 with corresponding Mach numbers of 0.08, 0.09, and 0.12, respectively. The stability derivatives were obtained from straight-line fairings of data obtained from tests at 0° and $\pm 5°$ angle of yaw. Extended angle-of-yaw tests were made at several angles of attack to cover the yaw range from -5° to 25° angle of yaw.

For the wing-alone tests the following flap configurations were used: (a) flaps neutral, (b) split flaps deflected, and (c) split flaps and leading-edge flaps deflected with fences installed. For the wing-fuselage tests only the first and third flap configurations were tested.

Air-stream surveys were made to determine the sidewash angles and dynamic pressures in a region approximating the location of a vertical tail. The surveys were made with the Langley 19-foot tunnel 6-tube rake (fig. 5) in a plane normal to the tunnel center line and 1.71$\bar{c}$ behind the center of gravity. (See fig. 6.) In some cases, the sidewash angles exceeded the values for which the rake had been calibrated and extrapolations of the calibrations were necessary. The extrapolated values are shown by the dot-dash lines in the figures. All tail surveys were made at a Reynolds number of 6.00×10^6.

CORRECTIONS TO DATA

The lift, drag, and pitching-moment data presented herein, have been corrected for support tare and interference effects and for air-stream misalinement. The jet-boundary corrections to the angle of attack and drag coefficient were calculated from reference 4, which accounts for wing sweep, and are as follows:

$$\Delta a = 0.94 C_L$$

$$\Delta C_D = 0.0139 C_L^2$$

The correction to the pitching-moment coefficient due to tunnel-induced distortions of the wing loading is:

$$\Delta C_m = 0.0064 C_L$$

All of these corrections were added to the data. No corrections were applied to the rolling-moment, yawing-moment, and lateral-force coefficients.

RESULTS AND DISCUSSION

The lift, drag, and pitching-moment characteristics for the wing with all flap configurations used are presented in figure 7. The lateral-stability parameters are given as functions of lift coefficient and are presented in figures 8 to 11.

In figures 12 to 15, the aerodynamic characteristics are presented as a function of the angle of yaw. The results of the air-stream surveys are shown in figures 16 to 19.

Lateral-Stability Parameters of the Plain Wing

Dihedral effect.- At a Reynolds number of 6.00×10^6, the effective-dihedral parameter C_{l_ψ} increased with increasing lift coefficient to a maximum value of 0.0043 at a C_L of 0.95. Further increases in lift coefficient caused a rapid decrease in C_{l_ψ}, which became negative at a C_L of 1.08. An examination of the C_{l_ψ} curve (fig. 8) showed that

a decrease in the slope of the curve began at a lift coefficient of about 0.53. Observations of tufts on the wing surface with the model yawed at 5° revealed that an outboard cross flow started at the tip of the trailing wing panel at a C_L of about 0.53 and with increasing lift coefficient moved inboard along the leading edge. In reference 3, a more complete flow survey showed that this type of flow along the leading edge occurred coincidentally with leading-edge separation and an increase in the lift-curve slope. The rapid decrease in C_{l_ψ} after it reached its maximum value was shown by the tuft studies to be caused by the spreading of the stall which began on the leading wing panel at a lift coefficient of about 0.90.

Directional stability and lateral force.- The plain wing had neutral directional stability at zero lift but gradually increased in stability with increasing lift coefficient up to a C_L of 0.70. Beyond this point, the directional stability decreased rapidly and the wing became directionally unstable at a C_L of 0.76. The instability seems to coincide with the decrease in the slope of the C_{l_ψ} curve. Although the wing became stable again at a C_L of 1.03, it was unstable at the maximum lift coefficient.

The lateral-force parameter C_{Y_ψ} was negligible at lift coefficients below 0.70 but varied from a negative value of about -0.0075 at a C_L of 0.87 to a positive value of about 0.007 at the maximum lift coefficient.

Effect of Flaps on the Lateral-Stability Parameters

Dihedral effect.- The initial rate of increase in effective dihedral with lift coefficient was slightly reduced by flap deflection. The maximum values of C_{l_ψ} were increased, however, to 0.0055 at a lift coefficient of 1.11 when the split flaps were deflected and to a value of 0.0065 at a C_L of 1.29 when both the split flaps and leading-edge flaps were deflected. The effective dihedral remained at a large positive value at the maximum lift coefficient when the leading-edge flaps were deflected; whereas with the plain wing and with only the split flaps deflected, C_{l_ψ} became negative at the maximum lift coefficient. (Tuft surveys showed that the leading-edge flaps delayed the tip stall.)

Directional stability and lateral force.- Flap deflection extended the range of lift coefficient in which the directional stability increased with increasing lift. With the split flaps deflected, the wing became

directionally unstable at a lift coefficient of about 0.95; and with both the leading-edge flaps and split flaps deflected, the wing became unstable at a C_L of 1.31. The large variations in directional stability and lateral force which occurred at high lift coefficients for the plain wing were apparent also when the split flaps were deflected but were minimized when the leading-edge flaps were deflected.

Fuselage Effects on the Lateral-Stability Parameters

Dihedral effect.- The lateral-stability parameters for the high-wing, low-wing, and midwing combinations are given in figure 9 for flaps neutral and in figure 10 for flaps deflected. The low-wing combination had less dihedral effect than the wing alone; but, as the wing position was progressively changed from low-wing to high-wing position, the dihedral effect increased. The increment of increase in C_{l_ψ} between the low-wing and midwing combinations was about equal to that between the midwing and high wing. The value of the increment in C_{l_ψ} at zero lift was about 0.0006 with flaps neutral and 0.0007 with the leading edge and split flaps deflected. The slopes of the C_{l_ψ} curves for the wing-fuselage combinations were slightly lower than for the wing alone for the flaps-neutral condition. The dihedral effect due to the midwing position was very small as had been expected. In general, the effects due to the fuselage were of the same magnitude as had been experienced on other sweptback and straight wings (references 1 and 5).

Directional stability and lateral force.- The fuselage decreased the directional stability of the plain wing by an increment in C_{n_ψ} which varied from about 0.0012 for the midwing combination to approximately 0.0015 for the low-wing combination. The increment in C_{n_ψ} was almost constant throughout the lift-coefficient range except when the leading edge and split flaps were deflected on the low-wing combination; then a large positive value of C_{Y_ψ} occurred at zero lift, reducing the destabilizing yawing moment of the fuselage. The value of C_{Y_ψ} decreased with lift coefficient, and at a C_L of about 0.75 this relieving effect became negligible.

The midwing combination had the least side force of the three combinations, whereas the low-wing combination had the greatest.

Effect of Scale on Lateral-Stability Parameters

A large scale effect was noted in the lateral-stability parameters for the plain wing when the Reynolds number was increased from 1.93×10^6 to 4.35×10^6, as shown in figure 11. (The scale effect in the range of Reynolds number from 4.35×10^6 to 6.00×10^6 was moderate for all the stability parameters, except for C_{l_ψ} at high lift coefficients.) The maximum value of C_{l_ψ} at a Reynolds number of 1.93×10^6 was about one-half its value at $R = 6.00 \times 10^6$ and occurred at a much lower lift coefficient. The directional stability and side force were affected in a similar manner.

A very similar effect of Reynolds number was observed for the 42° sweptback wing of reference 1, and consequently it appears advisable to exercise caution when using lateral-stability parameters obtained at low Reynolds numbers, especially in the moderate to high lift range on swept wings with conventional airfoil shapes.

When the leading-edge and split flaps were deflected, the scale effect was negligible throughout the range tested.

Characteristics in Extended Yaw Range

The largest deviations of the stability parameters at high yaw angles from those measured at small yaw angles were obtained in the C_{n_ψ} and C_{Y_ψ} variations at high angles of attack. At an angle of attack of 16.8° the various configurations with flaps neutral (fig. 13) showed a reversal in slope for the variation of the yawing moment with angle of yaw at an angle of yaw of about 10°, tending to make the model less unstable. At an angle of attack of 23.3° (fig. 15), the directional instability due to the fuselage increased rapidly between the yaw angles of 10° and 13° when the leading-edge and split flaps were deflected.

AIR-FLOW CHARACTERISTICS IN THE REGION OF A VERTICAL TAIL

It is pointed out in reference 6 and shown in reference 1, that the sidewash angles in the region of the vertical tail may be affected by the wing-tip vortices when an airplane of low aspect ratio is yawed, especially at high lift coefficients when the vortices are strong.

The results of the air-stream surveys (figs. 16 to 19) show that the sidewash angles due to yaw are appreciable at the higher lift coefficients even for the plain wing, but they are only very slightly more negative than those for the 42° sweptback wing of reference 1. The aspect ratio of the 42° sweptback wing was 3.94 as compared with 2.88 for the 52° sweptback wing discussed herein. The variation of the sidewash angles and dynamic pressure ratios at the tail with height above the fuselage center line were very similar to those for the 42° wing, indicating that the effect of the wing vortices is essentially the same for the two wings. Unfavorable sidewash and wake characteristics occurred at the high angles of attack for the high-wing combination, but these effects diminished as the wing position became lower. The greater height above the wing wake and the end-plate effect of the wing on the fuselage vortices (as explained in reference 5) caused the low-wing combination to have favorable sidewash near the fuselage and also at the higher points.

The effect due to deflecting the leading-edge flaps, and split flaps in combination with the fences was to reduce slightly the negative sidewash angles and to cause the decrease in q_t/q due to the wing wake to be more severe. This same effect due to flap deflection occurred on the 42° sweptback wing.

SUMMARY OF RESULTS

The results of an investigation of the aerodynamic characteristics in yaw of a 52° sweptback wing in combination with a fuselage may be summarized as follows:

1. The effective-dihedral parameter of the plain wing had a maximum value of about 0.0043 at a lift coefficient of 0.95 beyond which it decreased rapidly and became negative. The wing was directionally stable up to a lift coefficient of 0.76.

2. The combination of leading-edge flaps, split flaps, and fences extended the range of increase of effective-dihedral parameter with lift coefficient up to the maximum lift coefficient and increased the directional stability to higher lift coefficients. In all cases, however, the wing was directionally unstable near the maximum lift coefficient.

3. The low-wing and high-wing combinations had lower and higher dihedral effect, respectively, than the wing alone, and the magnitudes of the differences were comparable to those experienced on unswept wings.

4. With flaps neutral, a large scale effect occurred for the lateral-stability parameters in the range of Reynolds number from 1.93×10^6 to 4.35×10^6 and a very moderate effect in the range from 4.35×10^6 to 6.00×10^6. With the combination of leading-edge flaps, fences, and split flaps the scale effect was negligible.

5. The results of air-stream surveys showed that the most favorable sidewash characteristics for directional stability occurred for the low-wing combination and were about the same as those obtained on a 42° sweptback wing.

Langley Aeronautical Laboratory
National Advisory Committee for Aeronautics
Langley Field, Va.,

REFERENCES

1. Salmi, Reino J., and Fitzpatrick, James E.: Yaw Characteristics and Sidewash Angles of a 42° Sweptback Circular-Arc Wing with a Fuselage and with Leading-Edge and Split Flaps at a Reynolds Number of 5,300,000. NACA RM No. L7I30, 1947.

2. Salmi, Reino J., Conner, D. William, and Graham, Robert R.: Effects of a Fuselage on the Aerodynamic Characteristics of a 42° Sweptback Wing at Reynolds Numbers to 8,000,000. NACA RM No. L7E13, 1947.

3. Fitzpatrick, James E., and Foster, Gerald V.: Static Longitudinal Aerodynamic Characteristics of a 52° Sweptback Wing of Aspect Ratio 2.88 at Reynolds Numbers from 2,000,000 to 11,000,000. NACA RM No. L8H25, 1948.

4. Eisenstadt, Bertram J.: Boundary-Induced Upwash for Yawed and Swept-Back Wings in Closed Circular Wind Tunnels. NACA TN No. 1265, 1947.

5. House, Rufus O., and Wallace, Arthur R.: Wind-Tunnel Investigation of Effect of Interference on Lateral-Stability Characteristics of Four NACA 23012 Wings, an Elliptical and a Circular Fuselage, and Vertical Fins. NACA Rep. No. 705, 1941.

6. Recant, Isidore G., and Wallace, Arthur R.: Wind-Tunnel Investigation of the Effect of Vertical Position of the Wing on the Side Flow in the Region of the Vertical Tail. NACA TN No. 804, 1941.

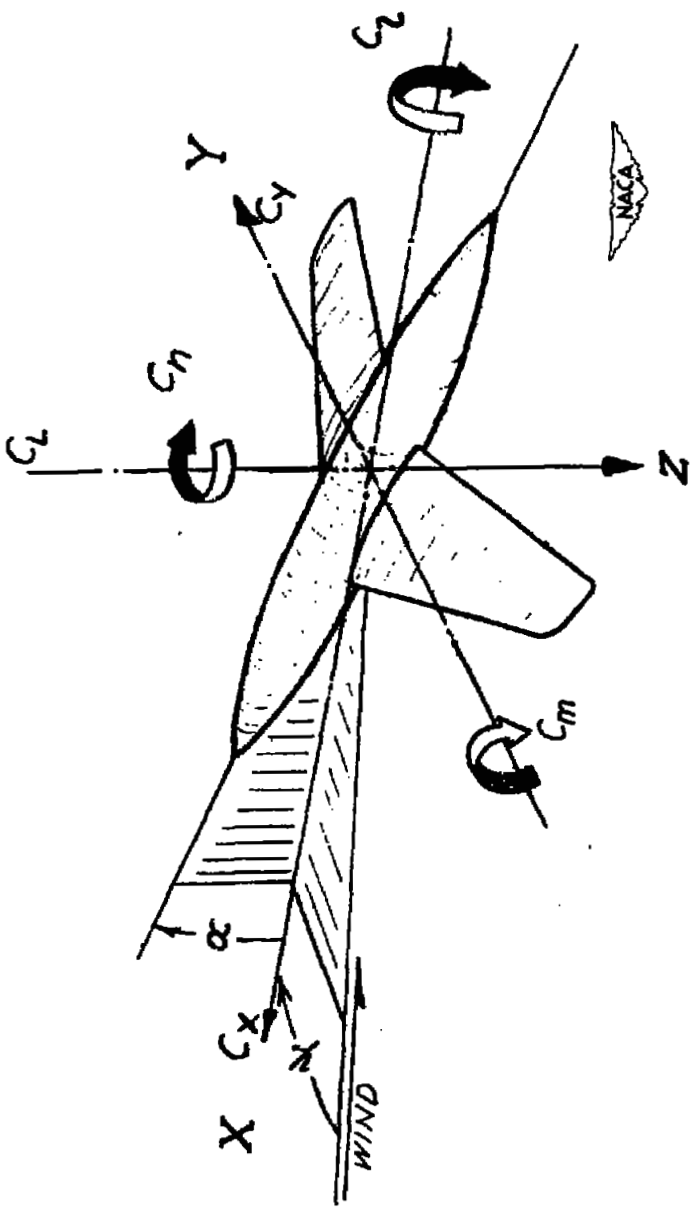

Figure 1.- System of axes. Arrows indicate positive directions.

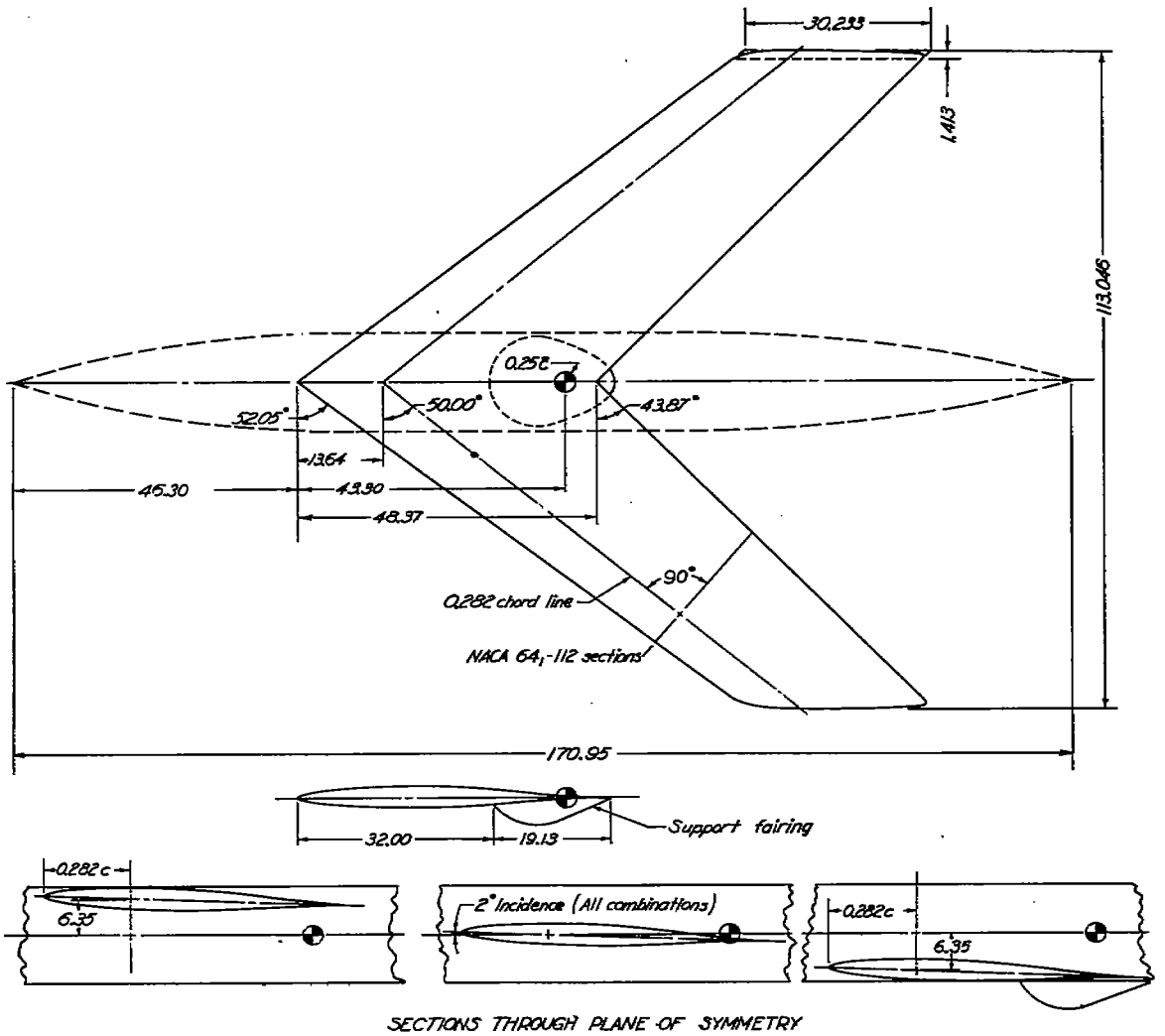

FUSELAGE ORDINATES

Distance from nose	Diameter	Distance from nose	Diameter
0	0.2	112.00	16.80
18.00	9.84	122.00	16.32
22.05	11.80	132.00	14.90
27.39	13.80	142.00	12.52
34.56	15.60	151.20	9.46
42.35	16.60	162.00	4.78
48.00	16.80	170.95	0.20

NACA

Figure 2.- Geometry of 52° sweptback wing and fuselage. Aspect ratio = 2.88; taper ratio = 0.625; area = 4429 sq in.; $\bar{c}$ = 39.97 in. No dihedral or twist. (All dimensions in inches.)

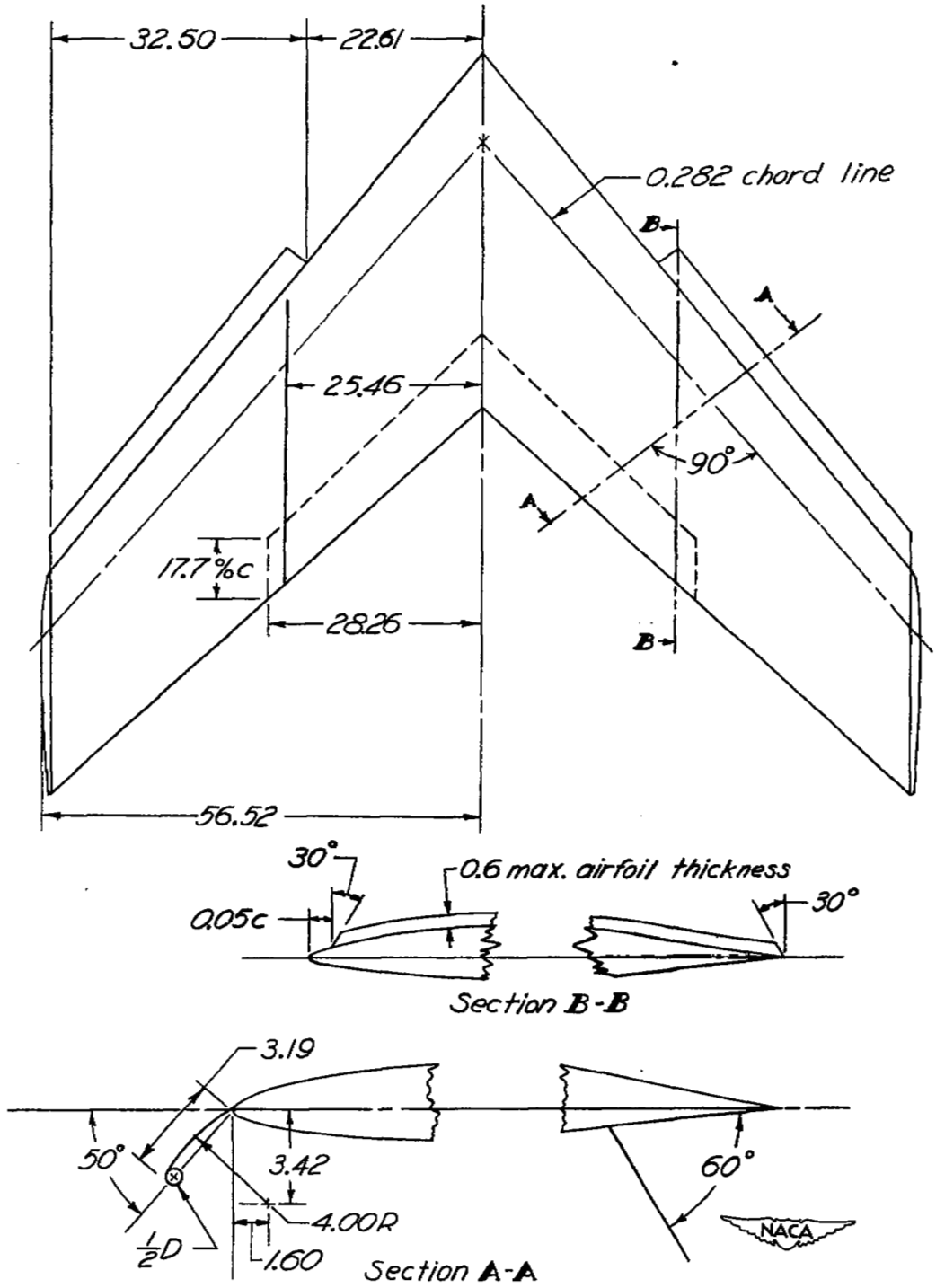

Figure 3.- Geometry of flaps and fences for the 52° sweptback wing. (All dimensions in inches.)

Figure 4.- 52° sweptback wing and fuselage mounted in the Langley 19-foot pressure tunnel. Low-wing configuration; flaps deflected.

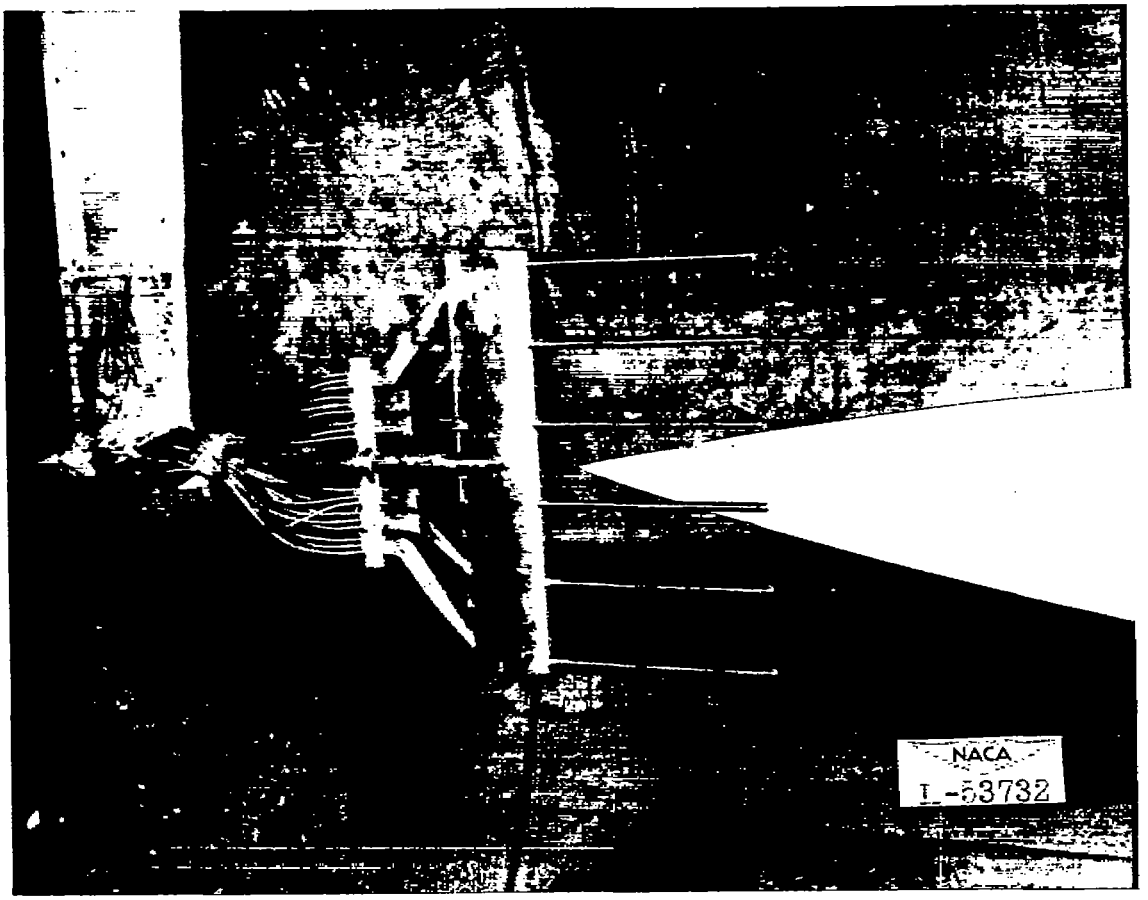

(a) Photograph of rake head.

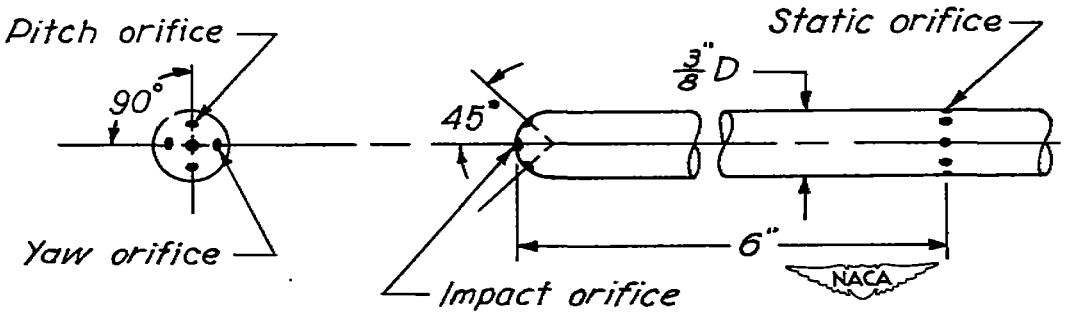

(b) Sketch of tube head.

Figure 5.- Langley 19-foot pressure tunnel air-stream survey rake.

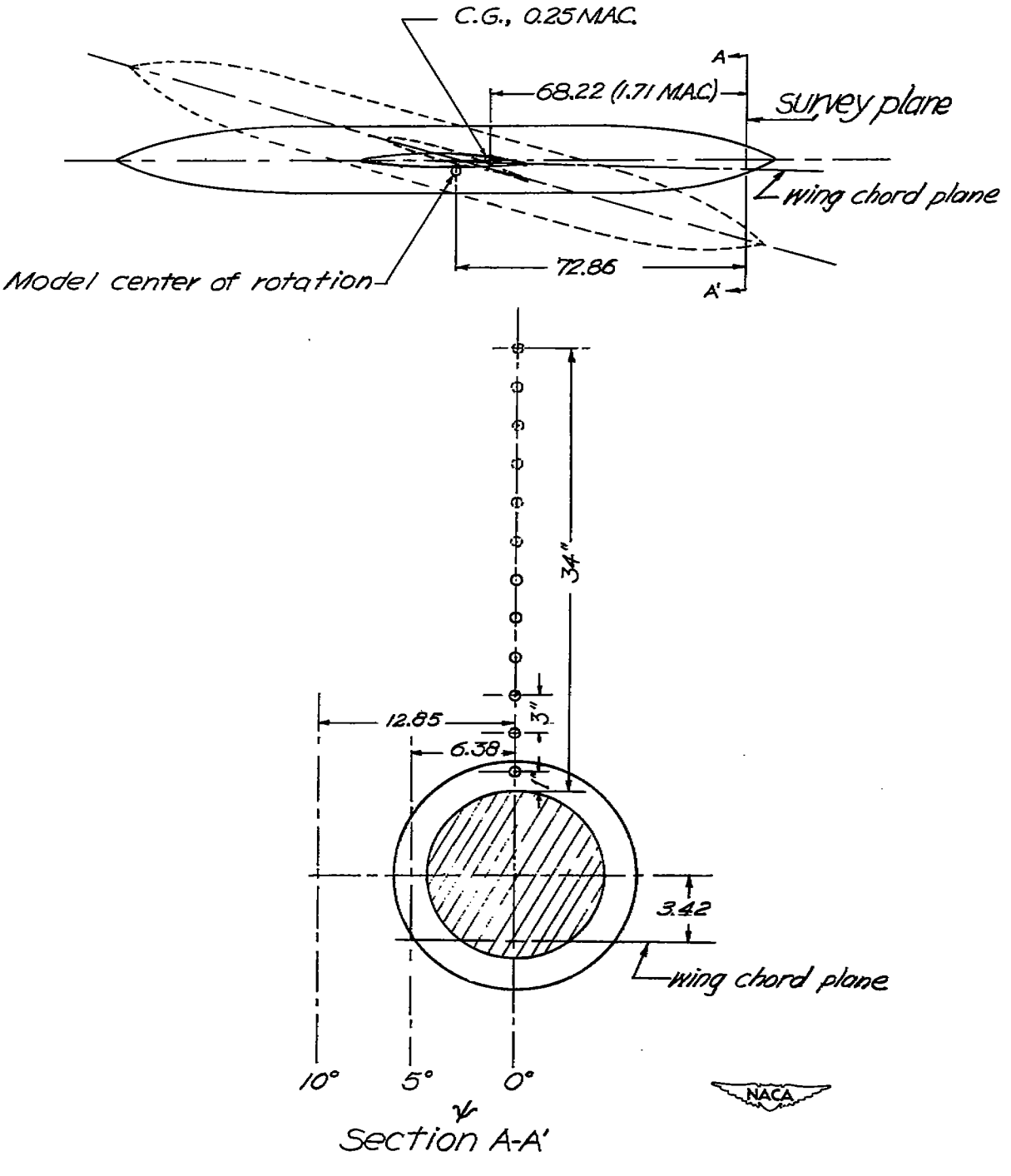

Figure 6.- Location of air-stream survey points.

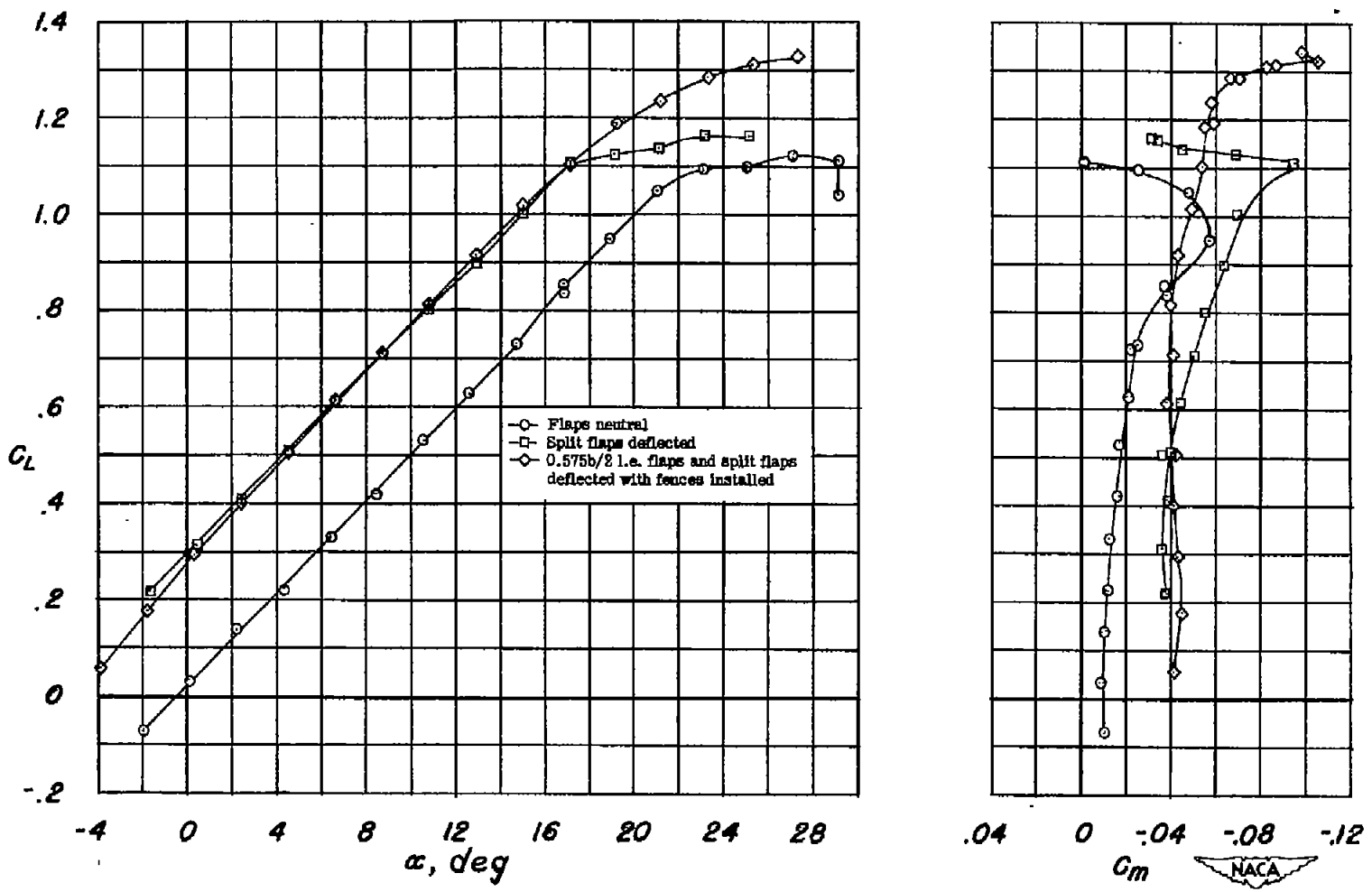

(a) C_L plotted against α and C_m.

Figure 7.- Longitudinal aerodynamic characteristics of a 52° sweptback wing with three flap configurations. R = 6.00 × 10^6.

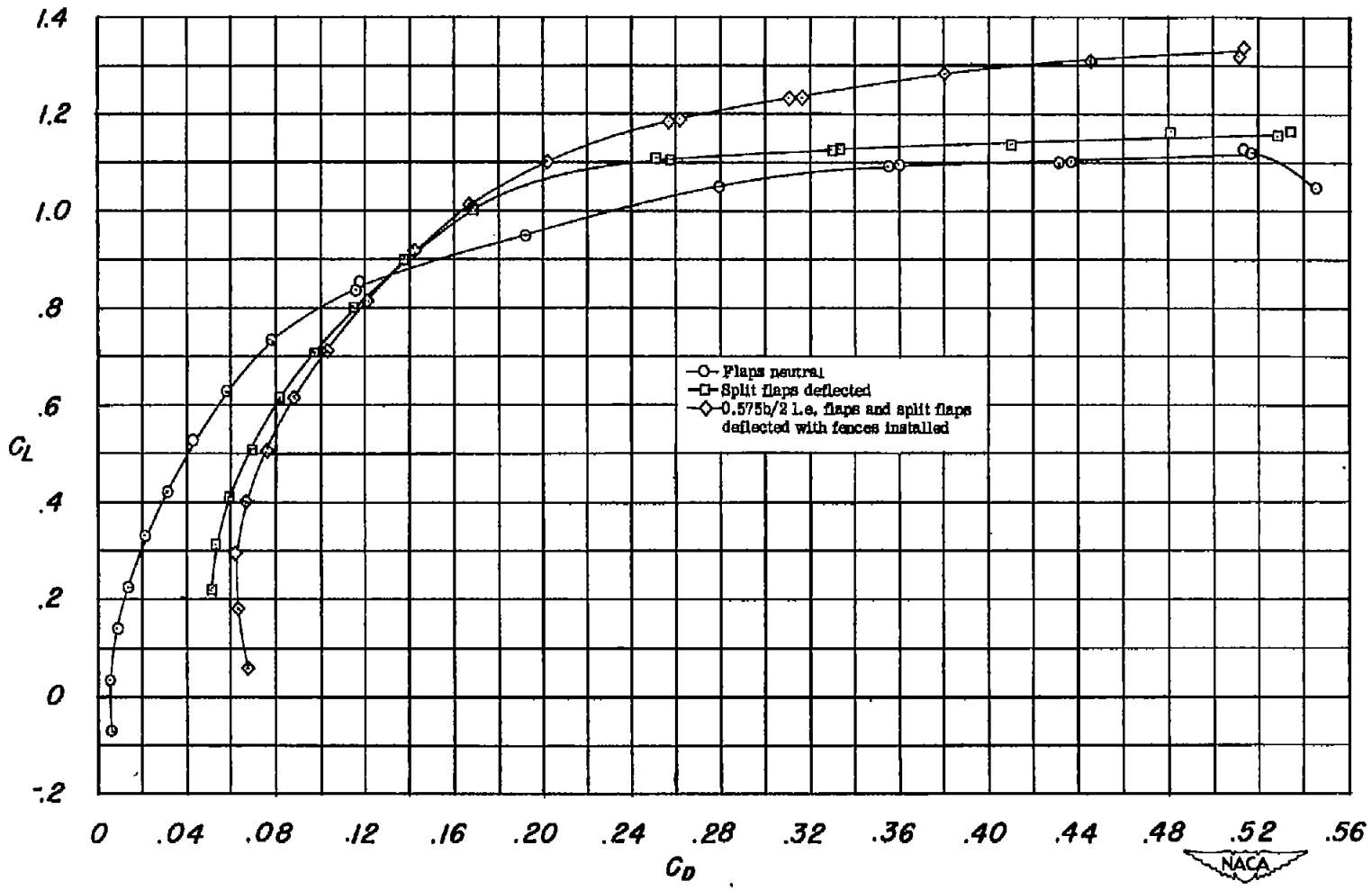

(b) C_L plotted against C_D.

Figure 7.-. Concluded.

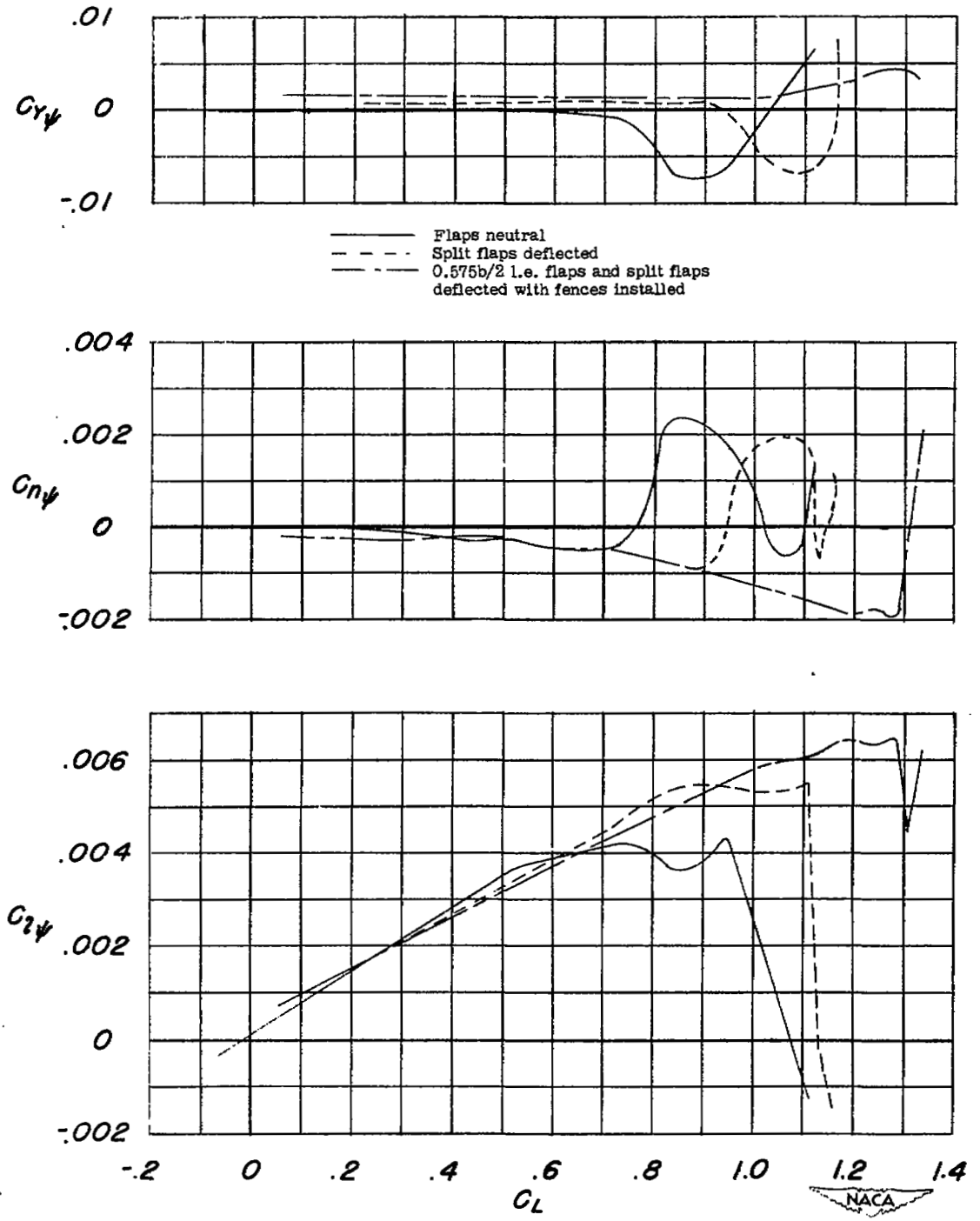

Figure 8.- Variation of C_{l_ψ}, C_{n_ψ}, and C_{Y_ψ} with C_L for a 52° sweptback wing with three flap configurations. R = 6.00 × 10^6.

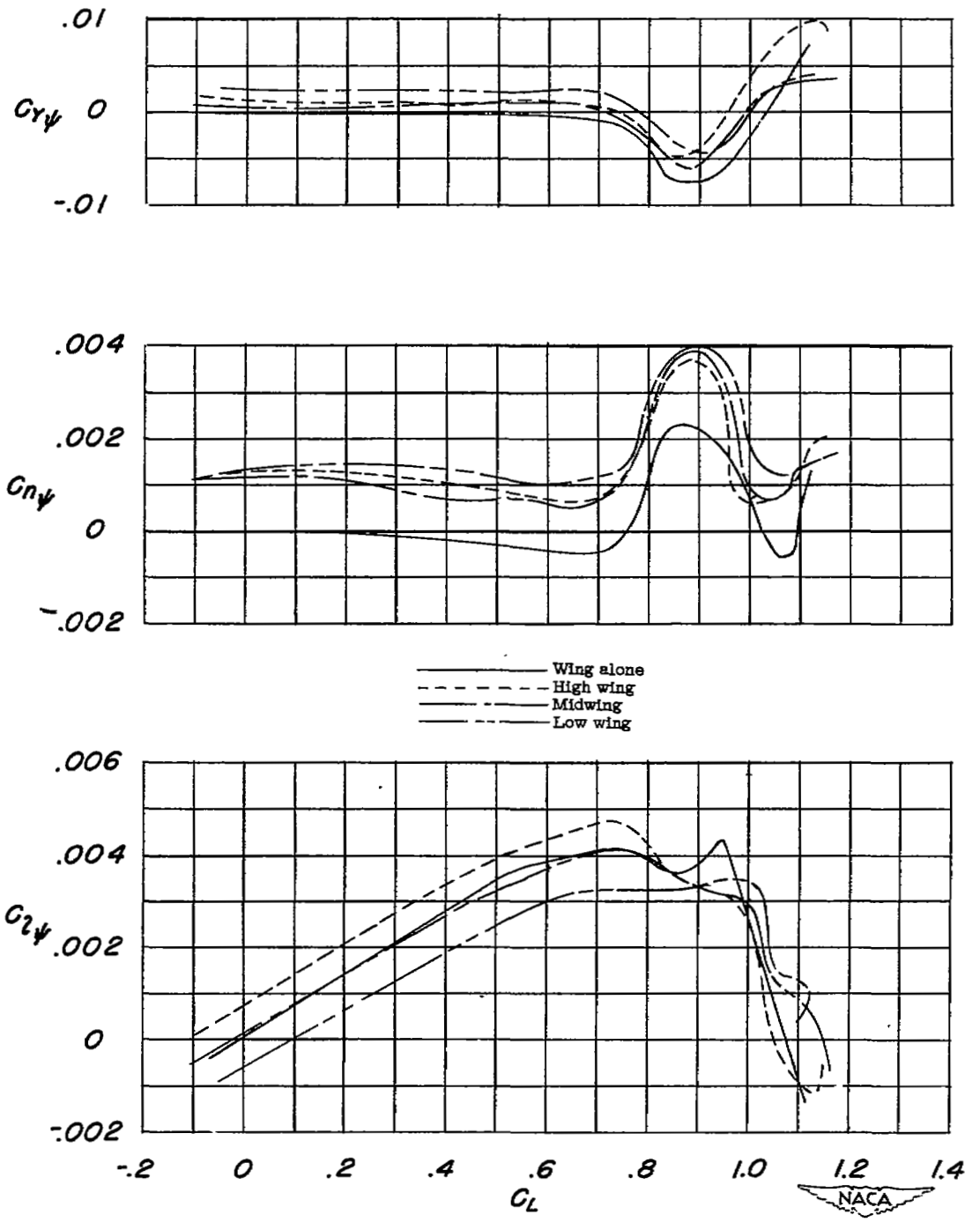

Figure 9.- Effect of wing-fuselage position on the variation of C_{l_ψ}, C_{n_ψ}, and C_{Y_ψ} with C_L for a 52° sweptback wing. Flaps neutral. $R = 6.00 \times 10^6$.

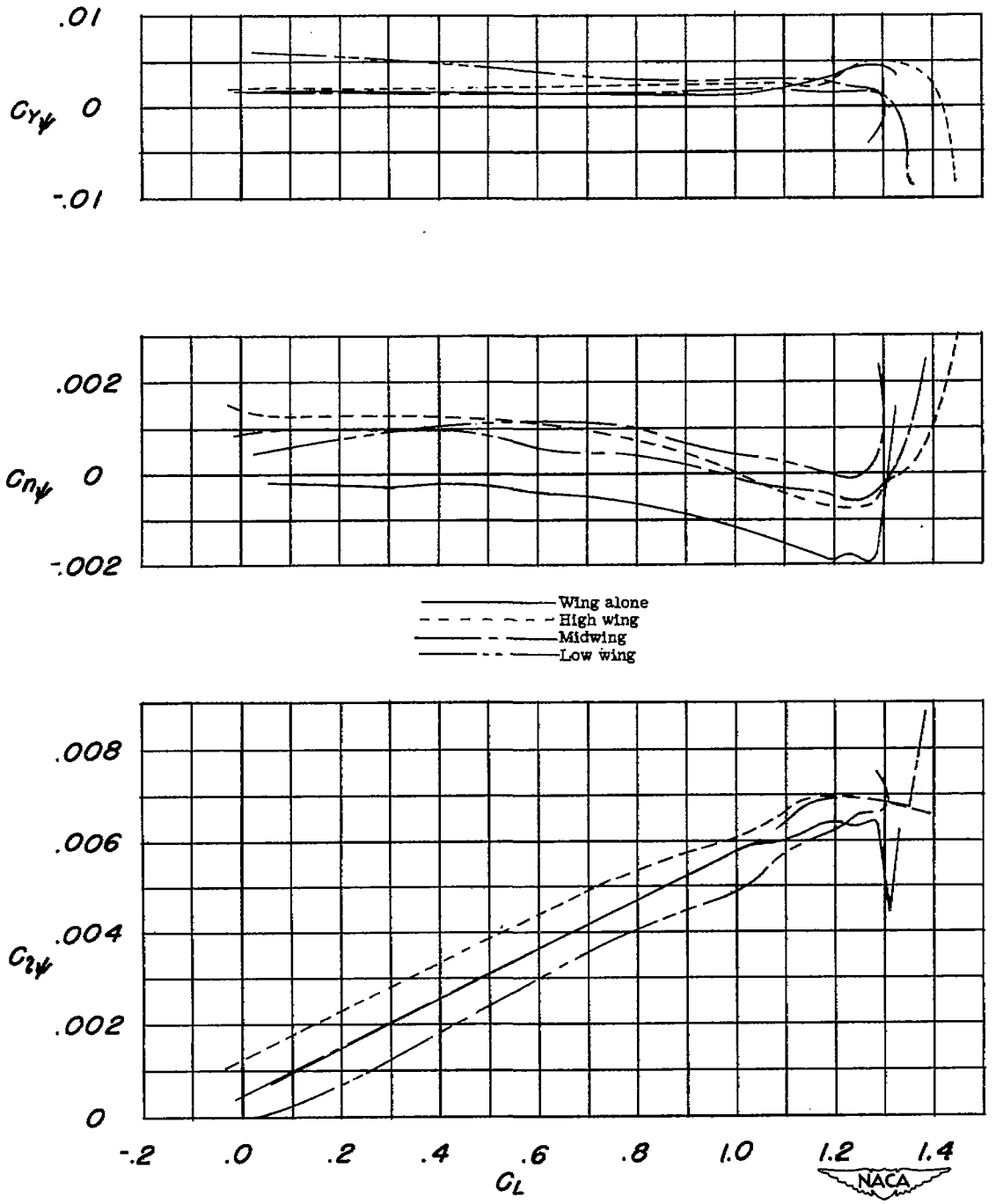

Figure 10.- Effect of wing-fuselage position on the variation of C_{l_ψ}, C_{n_ψ}, and C_{Y_ψ} with C_L for a 52° sweptback wing. 0.575 leading-edge flaps and split flaps deflected with fences installed. R = 6.00 × 10^6.

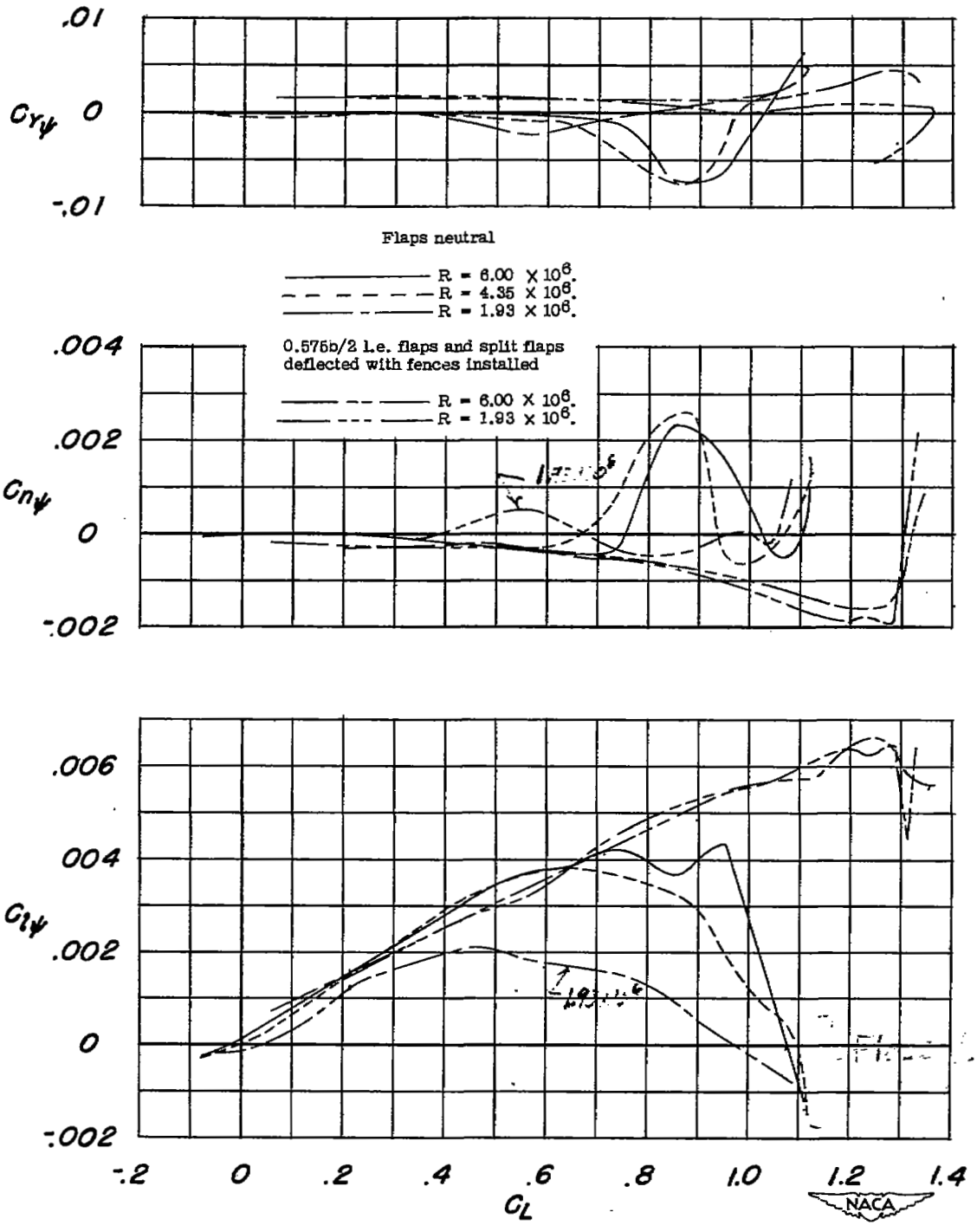

Figure 11.- Effect of Reynolds number on the variation of C_{l_ψ}, C_{n_ψ}, and C_{Y_ψ} with C_L for a 52° sweptback wing with two flap configurations.

LER = .010 c

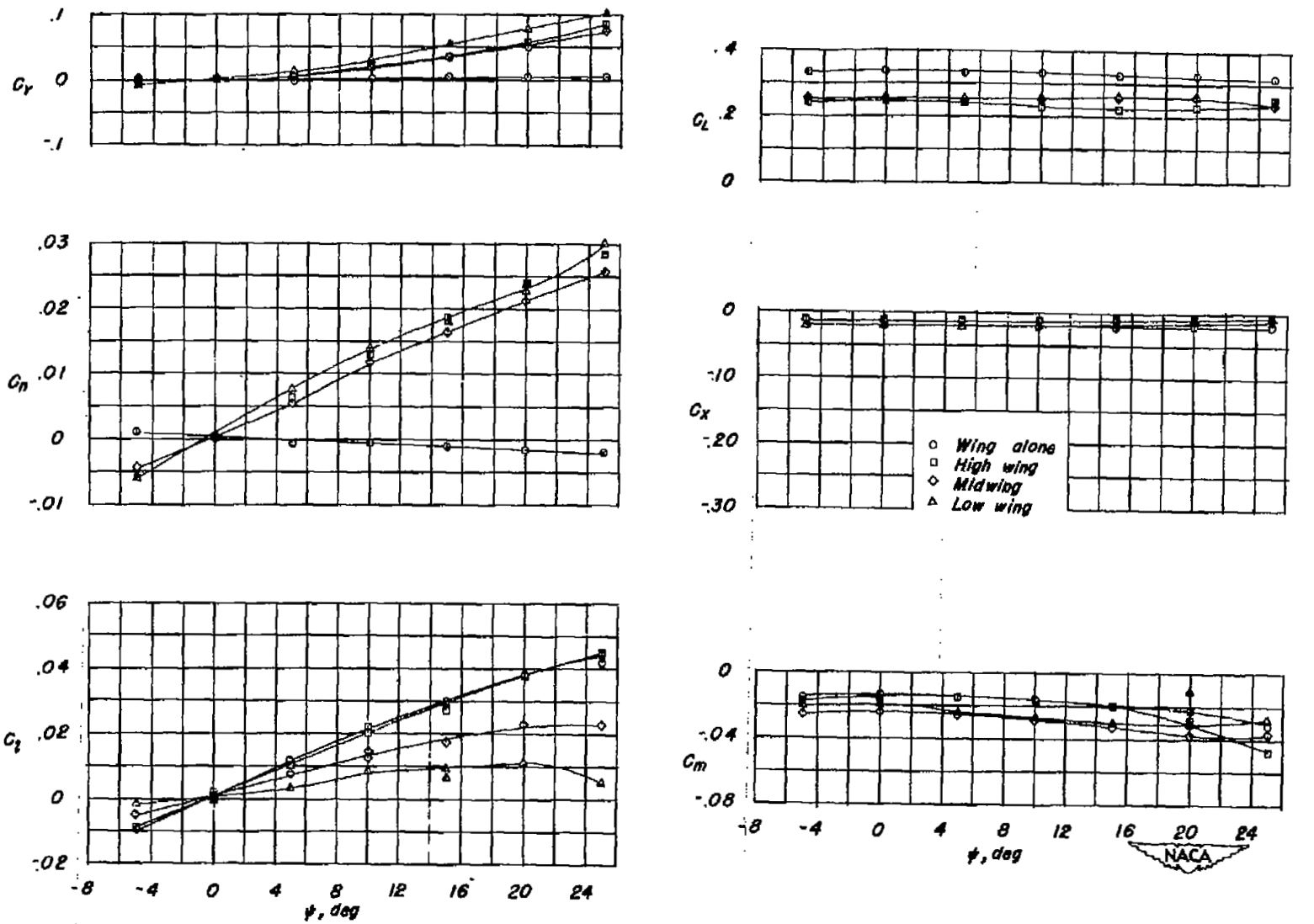

Figure 12.- Aerodynamic characteristics in yaw of a 52° sweptback wing, alone and in high wing, midwing and low wing combinations. Flaps neutral. $\alpha = 4.3^\circ$, except wing alone $\alpha = 6.4^\circ$. $R = 6.00 \times 10^6$.

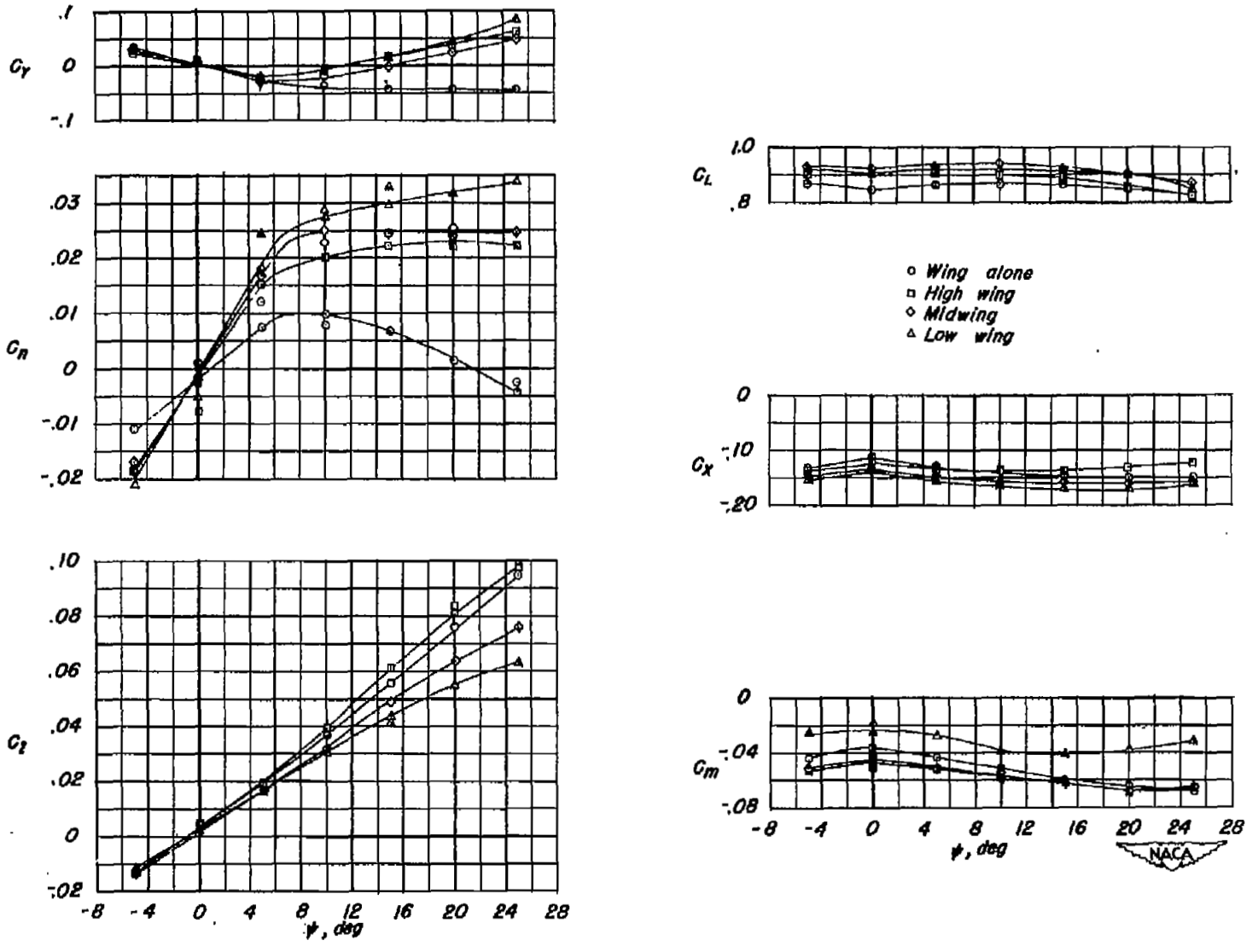

Figure 13.- Aerodynamic characteristics in yaw of a 52° sweptback wing alone and in high wing, midwing and low wing combinations. Flaps neutral, $\alpha = 16.8°$. $R = 6.00 \times 10^6$.

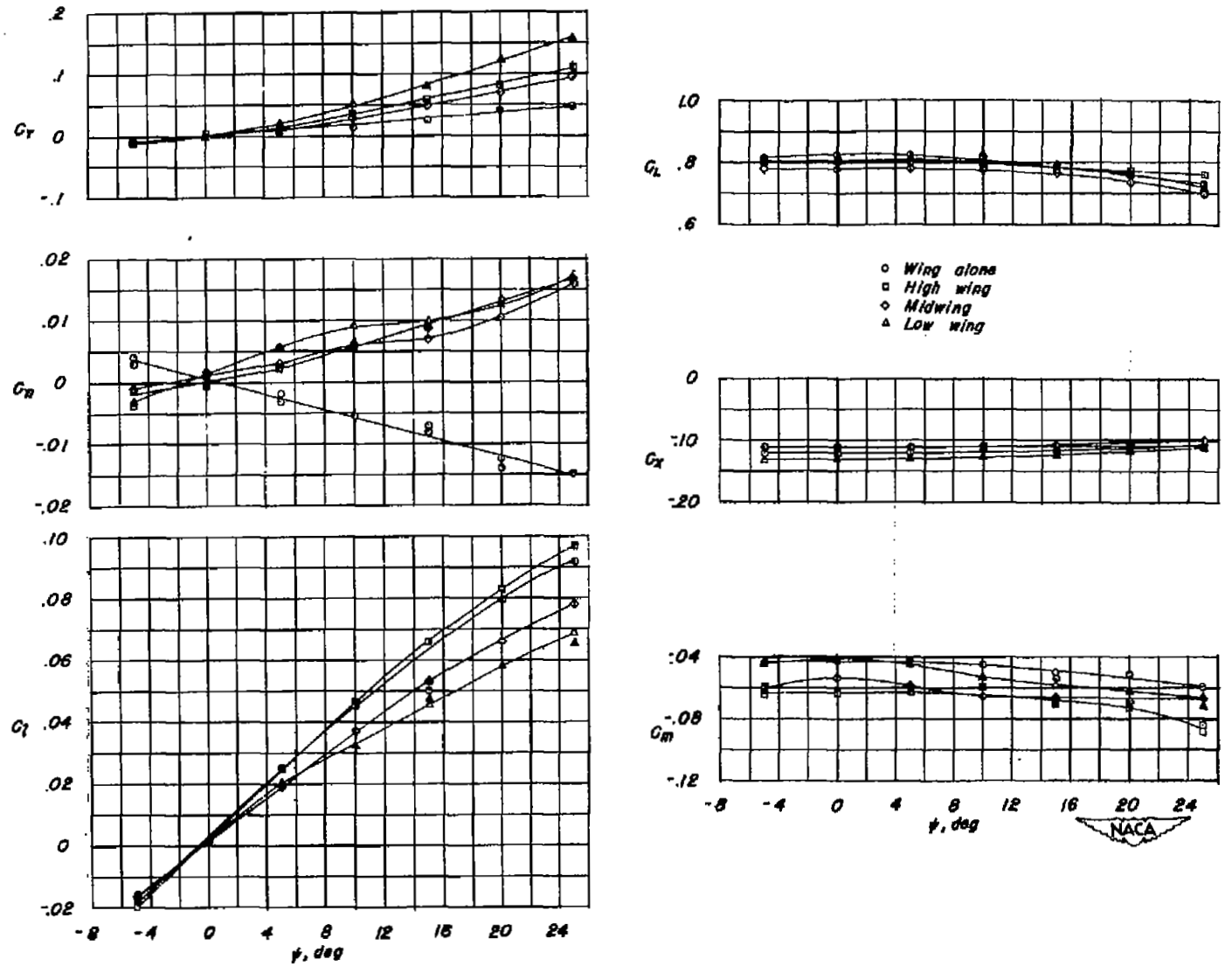

Figure 14.- Aerodynamic characteristics in yaw of a 52° sweptback wing alone and in high wing, midwing and low wing combinations. Leading-edge and split flaps deflected with fences installed, $\alpha = 10.8°$. $R = 6.00 \times 10^6$.

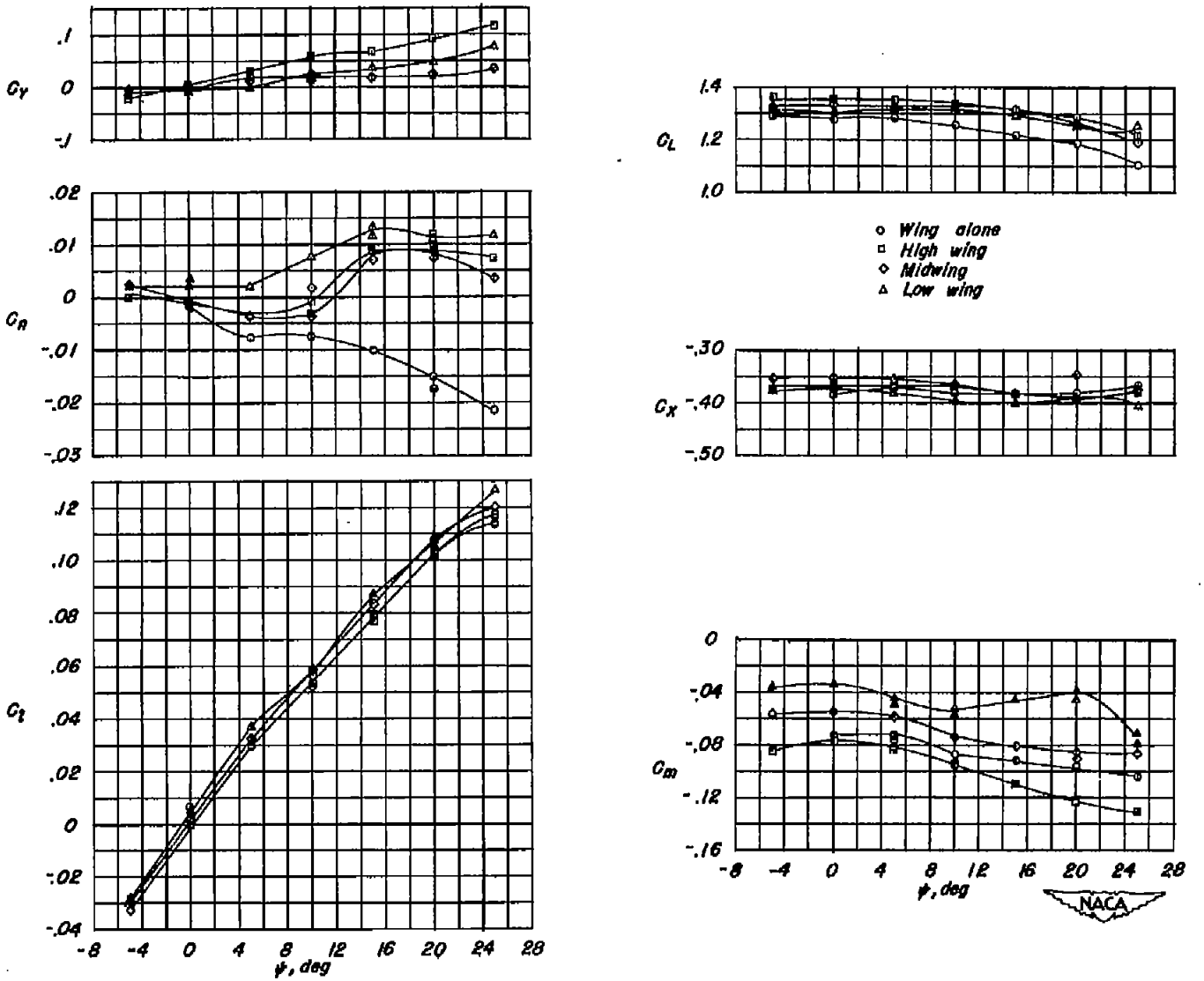

Figure 15.- Aerodynamic characteristics in yaw of a 52° sweptback wing alone and in high wing, midwing and low wing combinations. Leading-edge and split flaps deflected with fences installed, $\alpha = 23.3°$. $R = 6.00 \times 10^6$.

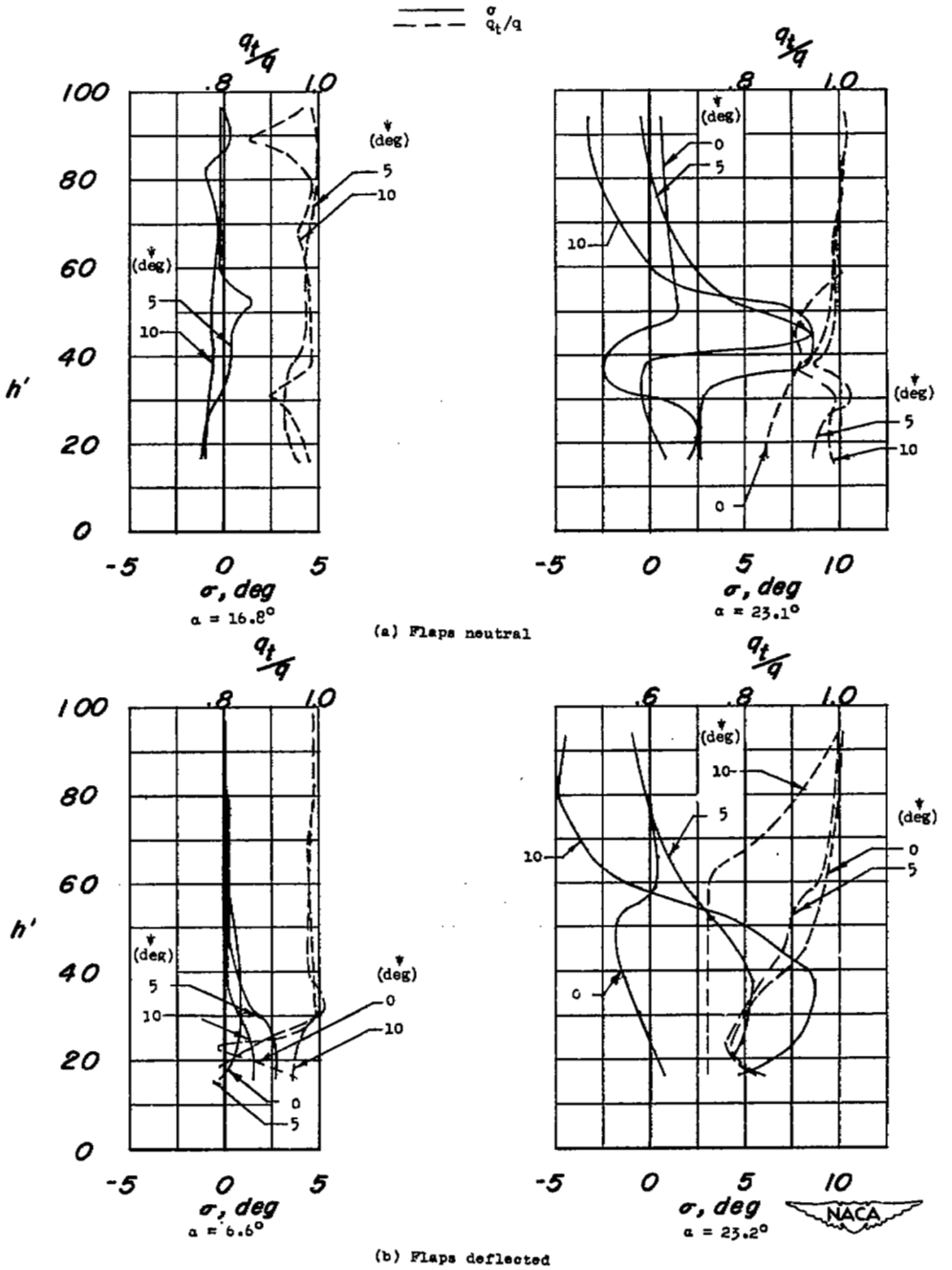

Figure 16.- Variation of sidewash angles and dynamic pressures at the vertical tail positions with height above wing chord plane, for various angles of yaw. Wing alone. R = 6.00 × 10^6.

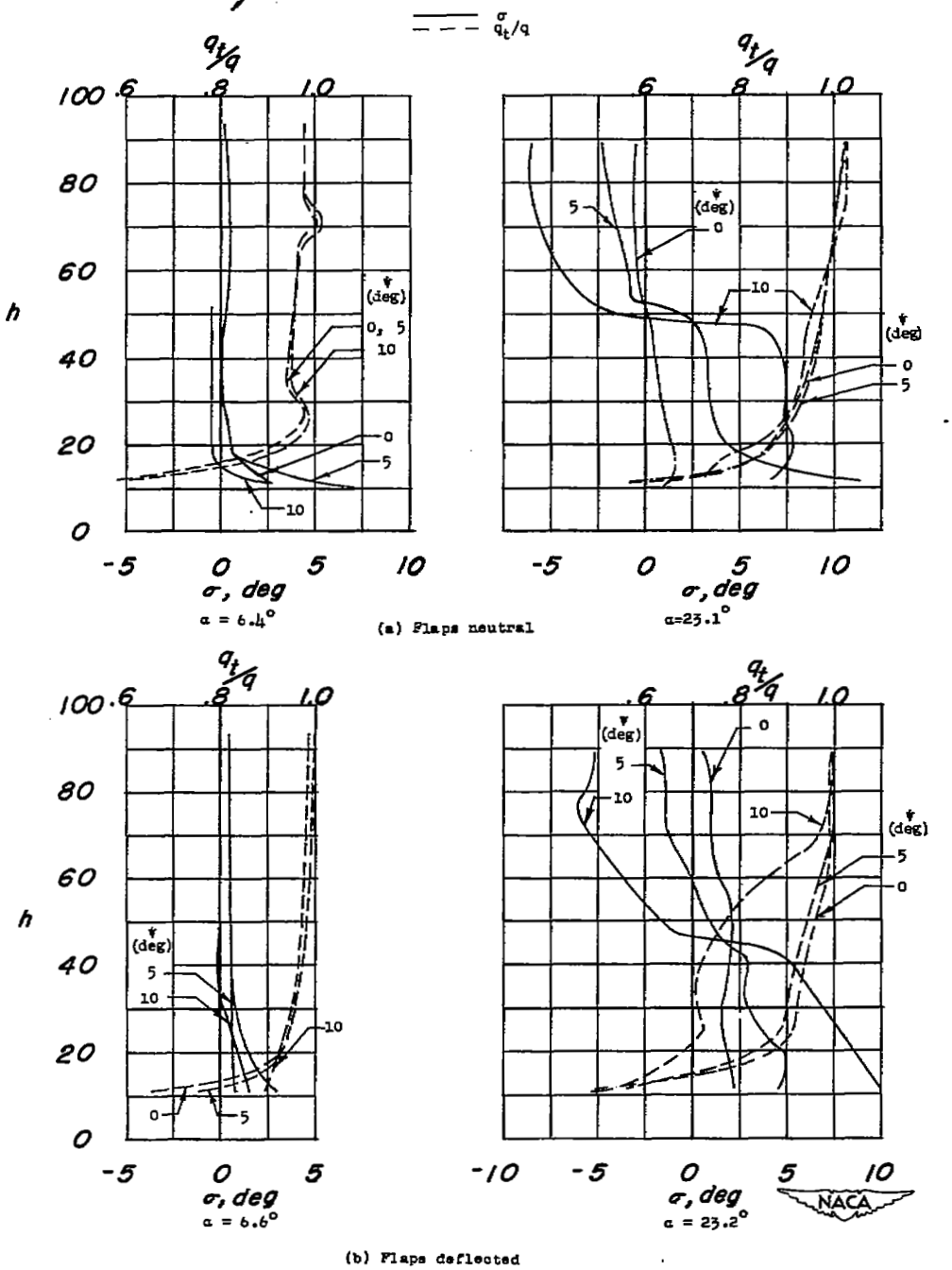

Figure 17.- Variation of sidewash angles and dynamic pressures at the vertical tail position with height above fuselage center line, for various angles of yaw. High-wing combination. R = 6.00 × 10^6.

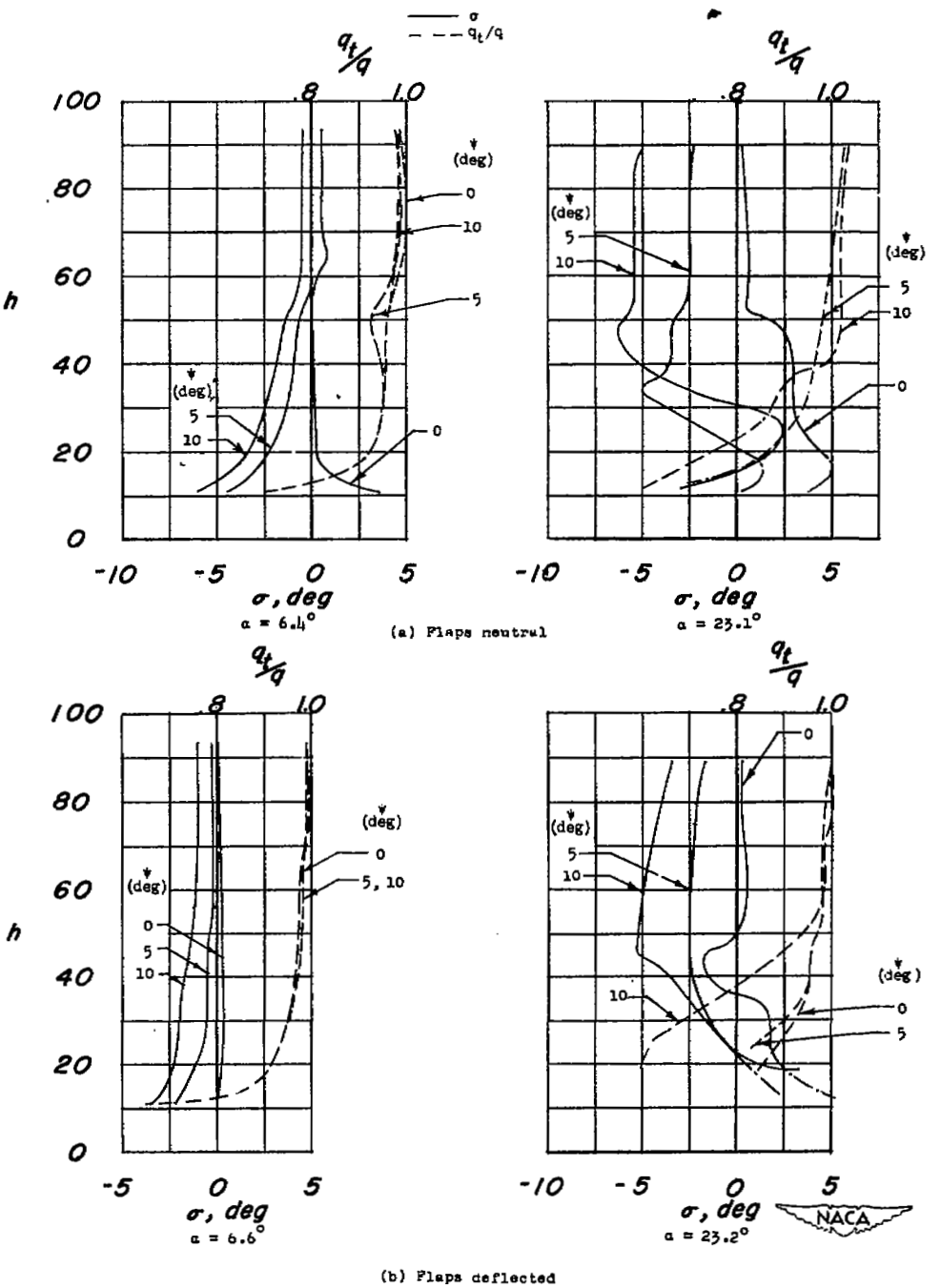

(a) Flaps neutral

(b) Flaps deflected

Figure 18.- Variation of sidewash angles and dynamic pressures at the vertical tail position with height above fuselage center line, for various angles of yaw. Midwing combination. R = 6.00 × 10^6.

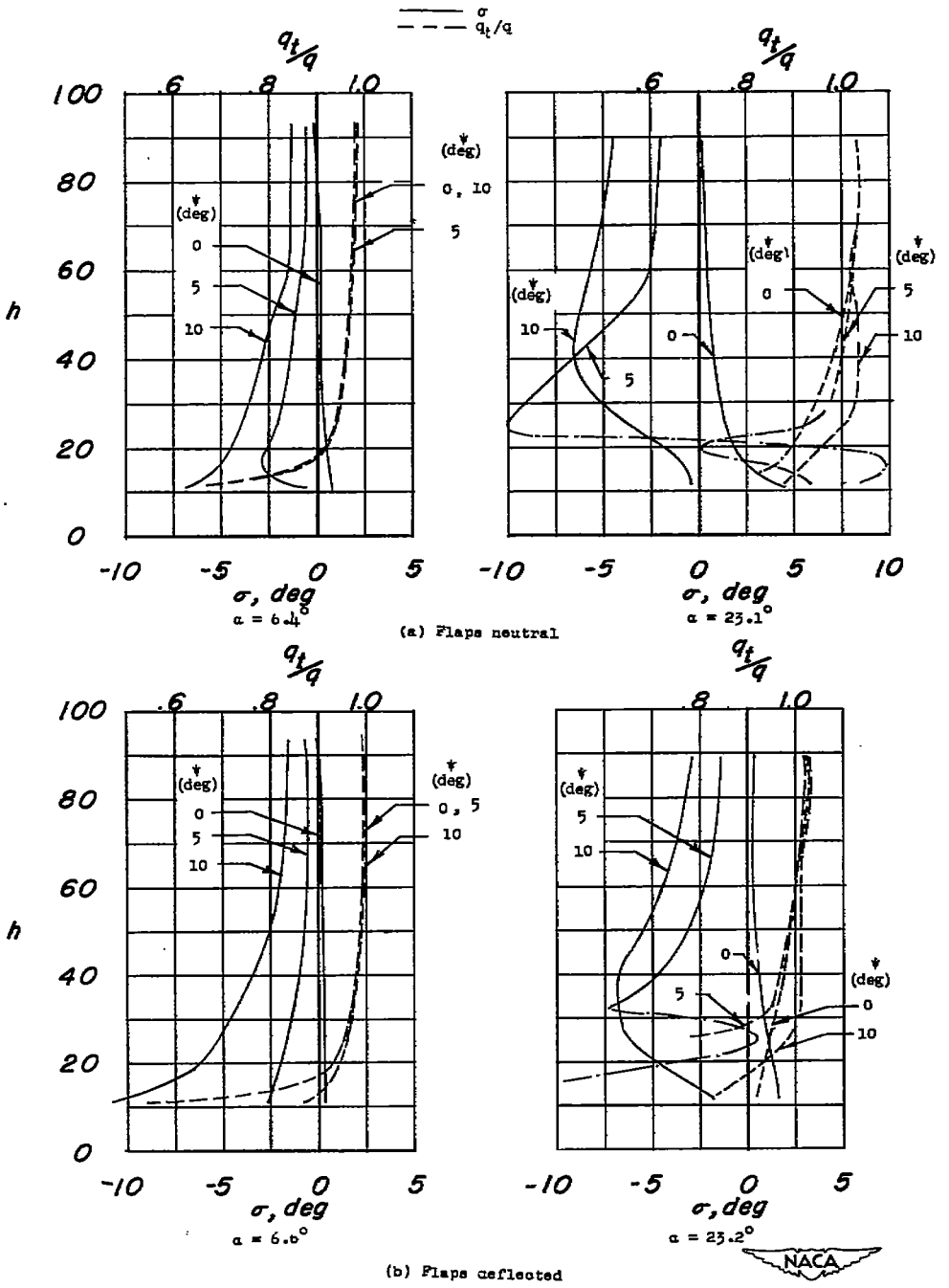

(b) Flaps deflected

Figure 19.- Variation of sidewash angles and dynamic pressure at the vertical tail position with height above fuselage center line. Low-wing combination. R = 6.00 × 10^6.